Advanced Vision-guided Robotic Tying with 6-DoF Rebar Pose Estimation

Mi Liu[1], Jingjing Guo[1,2], Lu Deng[1,2,*], Xiaoyi Lyu[1], Linzhen Nie[3]

[1]College of Civil Engineering, Hunan University, China
[2]Key Laboratory of Damage Diagnosis for Engineering Structures of Hunan Province, Hunan University, China
[3]School of Automotive Engineering, Wuhan University of Technology, China
*Corresponding Author
liumi@hnu.edu.cn, guojingjing@hnu.edu.cn, *denglu@hnu.edu.cn, lyuxiaoyi@hnu.edu.cn, linzhen_nie@whut.edu.cn

Abstract –

Rebar tying is a time-consuming and labor-intensive process that involves repetitive bending and hand motions to secure rebar with wire, often leading to muscular and skeletal injuries. To address these challenges, rebar tying robots have been developed to automate the process. However, existing studies primarily focus on tying point localization for horizontal rebar mesh, neglecting the 6 Degrees of Freedom (DoF) pose estimation necessary for tying complex reinforcement skeletons where rebar may be arranged in various spatial orientations. Therefore, this study proposes a 6-DoF rebar pose estimation method based on keypoint detection and point cloud registration. A deep learning-based keypoint detection algorithm is employed to extract point cloud data from each rebar intersection. Additionally, to tackle challenges posed by texture-less and self-occluding features of rebar point clouds, a coarse registration method utilizing geometric features and a fine registration method based on adaptive displacement correction is introduced to ensure accuracy and stability in rebar pose estimation. The proposed method enables the robot to autonomously understand the relative spatial relationship between itself and the tying objects, facilitating precise tying across a broader range of reinforcement skeletons, thereby significantly reducing the demand for manual labor.

Keywords –
Rebar tying; Rebar pose estimation; Keypoint detection; Point cloud registration; Reinforcement skeleton.

1 Introduction

Rebar tying is a crucial process in reinforced concrete construction. Its primary purpose is to secure the position of rebar, ensuring that it remains correctly positioned according to the design drawings during concrete pouring. However, manual rebar tying is a labor-intensive task that requires workers to bend repeatedly and tie each rebar crosspoint by hand [1].

To overcome this problem, vision-guided robotic systems have been applied to automate rebar tying tasks in recent years. For example, Tybot [2], a gantry-mounted tying robot shown in Figure 1 (a), navigates along the screed or porta-rail and uses a dual-camera system to extract tying information for bridge deck operations. Similarly, the rebar tying robot developed by the Beijing Institute of Technology [3], as shown in Figure 1 (b), moves steadily in four directions across the rebar mesh and employs a vision system to detect crosspoints and guide the tying process. A similar robot, T-iROBO [4], is shown in Figure 1 (c). In both types of robots, the vision system plays a critical role in tying operations by extracting spatial information about tying points through visual perception technology, thereby guiding the robot to complete tying tasks efficiently.

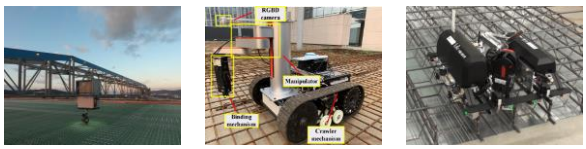

(a) (b) (c)

Figure 1. Rebar tying robots: (a) Tybot [2], (b) the rebar tying robot developed by the Beijing Institute of Technology [3], (c) T-iROBO [4].

For tying information extraction in the vision systems of rebar tying robots, Jin et al. [3] proposed using a deep learning-based keypoint detection algorithm to identify pixel coordinates of the rebar crosspoint and then calculate the rebar crosspoint's spatial coordinates by integrating the depth value of the point. Similarly, Cheng and Deng [5] introduced a rebar crosspoint recognition

method based on MobileNetV3 and the SSD algorithm. Previous research on rebar tying robots has primarily focused on detecting rebar crosspoints, enabling the robotic arm to perform three linear motions to position the end effector at the tie point. However, estimating the tying orientation has been less explored, despite its importance in guiding the end effector to rotate to the appropriate angle. This ensures that the tying wire correctly wraps around the rebar and facilitates subsequent tying operations. In construction practice, rebar planes are often positioned in various orientations on construction sites, such as the reinforcement skeletons of beams and walls, which can be vertical or inclined as well as horizontal. In these scenarios, a robotic arm with at least 6 Degrees of Freedom (DoF) is typically required to perform 6-DoF tying operations, enabling flexible positioning and orientation to meet complex rebar tying requirements. Consequently, merely detecting tying position information in previous research is insufficient for addressing rebar tying tasks in reinforcement skeletons, and it is desired to develop advanced vision perception methods to enable rebar tying robots to adapt to various spatial configurations and perform 6-DoF tying operations effectively.

Object pose estimation plays a crucial role in 6-DoF robotic manipulation, enabling robots to determine the spatial position and orientation of objects for accurate task execution [6]. Traditional methods determine the object pose by aligning the template point cloud with the scene point cloud using point cloud registration techniques [7]. The Iterative Closest Point (ICP) algorithm is one of the most commonly used point cloud registration methods for object pose estimation. It is typically employed to refine the pose after an initial rough estimate, as ICP is prone to get trapped in local optimal without a good starting pose [7]. Coherent Point Drift (CPD) is another widely used registration method capable of handling rigid, non-rigid, and affine transformations, making it suitable for pose estimation of deformable objects like cables and ropes [8,9]. Additionally, feature-based registration techniques, including point feature histograms (PFH) and fast point feature histograms (FPFH) have also been adapted for object pose estimation [10]. However, despite their widespread use, traditional methods exhibit limitations when applied to texture-less objects, as similar surface features can lead to incorrect matches between corresponding and non-corresponding points during the registration process [11]. Rebar point cloud models often exhibit texture-less surfaces, and occlusions caused by outer rebar obscuring inner rebar further complicate point cloud registration. These challenges increase the risk of inaccurate rebar pose estimation, potentially leading to collisions between the robot and the rebar. Therefore, there is a pressing need for a novel rebar pose estimation method capable of addressing the challenges posed by texture-less and self-occluding features to enhance the accuracy of robotic tying operations.

To enhance the robot's capability to perform tying operations on complex reinforcement skeletons, where rebar may be arranged in various spatial orientations, this paper proposes a rebar pose estimation method that using deep learning-based keypoint detection and point cloud registration. The proposed method includes several key innovations: (1) Introducing a tying point localization method based on keypoint detection, generating input data with prior displacement information. (2) Proposing a coarse-to-fine registration approach to handle texture-less and self-occluding rebar point clouds for rebar pose estimation. This innovative method enables the robot to adapt to diverse spatial configurations of the reinforcement skeleton and perform tying operations from various orientations and positions.

2 Method

To apply robotic rebar tying technology to diverse reinforcement skeletons in three-dimensional (3D) space, this paper develops a rebar pose estimation method to guide a 6-DoF robot in performing flexible tying operations from various orientations and positions. As shown in Figure 2, the proposed method comprises three modules: data generation, coarse registration, and fine registration. The data generation module functions as a preprocessing component, generating input data and prior displacement information for rebar pose estimation. The coarse registration and fine registration modules implement a coarse-to-fine point cloud registration method to address the challenges of texture-less and self-occluding, enabling accurate alignment of the template point cloud from the template frame to the camera frame for precise rebar position estimation. A detailed explanation is provided below.

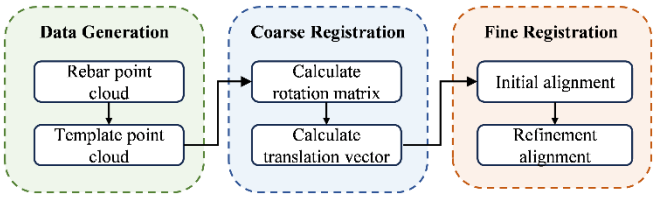

Figure 2. Flowchart of proposed formwork

2.1 Data Generation

2.1.1 Rebar Point Cloud

Keypoint detection is a critical task in computer vision, aimed at identifying essential features such as edges, corners, and textured areas within images or videos. In this study, the recently proposed deep learning-based keypoint detection model YOLOv8 [12] is employed to generate rebar point cloud data and extract the coordinate information of tying points for rebar pose estimation. This is achieved by detecting the bounding boxes and rebar crosspoints, followed by extracting the point cloud from the depth map of the tying area.

Reinforcement skeletons often contain multiple rebar layers at varying depths, presenting a visual challenge for keypoint detection algorithms in accurately identifying the top-layer crosspoints. To mitigate visual interference from rebars at different depths, this study uses a preprocessing technique [13] that applies a point cloud plane fitting algorithm to segment the point cloud at various depths and extract data corresponding to the nearest plane. The resulting point cloud data is transformed into a 2D color image containing only the pixels from the top-layer rebar. By focusing exclusively on the relevant layer, the preprocessing step facilitates accurate localization of tying points on the top layer, ensuring precise coordinate and point cloud data in the crosspoint area. Throughout this paper, the rebar point cloud in the area of the rebar crosspoint is referred to as the "rebar point cloud".

2.1.2 Template Point Cloud

Traditional object pose estimation method determines the pose of an object by aligning a template point cloud, which represents the object's shape and geometric features, with the object point cloud using point cloud techniques. In this study, the template point cloud used for rebar pose estimation is designed based on the typical layout of two intersecting cylindrical rebars in the tying area. The rebar length in the template point cloud is set to *3d*, where *d* is the diameter of the largest rebar in the intersection. Furthermore, to ensure a clear interpretation of registration results, the template's coordinate frame is aligned with the camera's coordinate frame with the Z-axis normal to the rebar plane and the X- and Y-axes aligned with the horizontal and vertical rebars, respectively.

2.2 Coarse Registration

The goal of the coarse registration module is to achieve a rough alignment between the template point cloud and the rebar point cloud. As shown in Figure 3, this is accomplished by determining the appropriate rotation matrix R and translation vector t based on the geometric feature of the rebar point cloud.

The rotation matrix R is computed by aligning the template point cloud parallel to the rebar point cloud using the normal vectors of the planes associated with both point clouds. Let n_t and n_r represent the normal vectors of the planes corresponding to the template point cloud and the rebar point cloud, respectively. In this study, we assume that n_t=(0,0,1). The normal vector n_r can have two possible orientations, which can result in different rotation axes and angles. To ensure consistent alignment, we control the orientation of n_r by ensuring its Z-component is positive, thereby aligning it with n_t. The rotation angle and axis can then be uniformly determined using the following equations:

$$n_r^{'} = \begin{cases} n_r, if\ (n_r)_z > 0 \\ -n_r, if\ (n_r)_z < 0 \end{cases} \tag{1}$$

$$\theta = \arccos\left(\frac{|\, n_r^{'} n_t \,|}{\| n_r^{'} \| \| n_t \|}\right) \tag{2}$$

$$k = \frac{n_t \times n_r^{'}}{\| n_t \times n_r^{'} \|} \tag{3}$$

where $(n_r)_z$ represents the Z-component of the vector n_r, θ refers to the rotation angle from n_t to $n_r^{'}$, and k represents the rotation axis vector. To determine the desired rotation matrix, an extended Rodrigues vector rotation formula is employed, which is widely utilized to describe rotations involving known rotation axes and specified angles [14].

$$R = E\cos\theta + (1-\cos\theta)\begin{pmatrix} k_x \\ k_y \\ k_z \end{pmatrix}(k_x, k_y, k_z) + \sin\theta \begin{pmatrix} 0 & -k_z & k_y \\ k_z & 0 & -k_x \\ -k_y & k_x & 0 \end{pmatrix} \tag{4}$$

where k_x, k_y and k_z denote the three components of the rotation axis k.

Furthermore, the translation vector t is determined by the difference in spatial coordinates between the tying point in the rebar point cloud, calculated from the pixel coordinates $p_r(u,v)$ predicted by YOLOv8, and the corresponding predefined point P_t.in the template point cloud. To obtain the spatial coordinate of the tying point in the rebar point cloud, pixel coordinates $p_r(u,v)$ are converted into spatial coordinates $P_r(X,Y,Z)$ using the following formula:

$$\begin{pmatrix} X \\ Y \\ Z \end{pmatrix} = d \cdot K^{-1} \cdot \begin{pmatrix} u \\ v \\ 1 \end{pmatrix} \quad (5)$$

where d is the depth value of tying point, and K represents the camera intrinsic matrix. The translation vector t can be calculated as:

$$t = P_r - R \cdot P_t \quad (6)$$

2.3 Fine Registration

To further enhance the registration accuracy, the point-to-plane ICP method [15] is employed to minimize the alignment errors between the template point cloud and the rebar point cloud during fine registration. Upon completion of the registration process, the ICP algorithm yields the transformation matrix that aligns the roughly registered template point cloud with the rebar point cloud, ensuring precise alignment for subsequent processing tasks. However, the rebar point cloud often exhibits uneven density between the inner and outer rebar due to self-occlusion, which can cause the registration algorithm to prematurely converge to a local optimum. This typically occurs when the outer rebar is aligned, leaving the sparser inner rebar unaccounted for. To address this issue, an adaptive displacement correction strategy is designed to help the algorithm escape from local optima, as shown in Figure 3. Specifically, after the initial fine registration using point-to-plane ICP, the registration quality is evaluated based on the root mean square error (RMSE) threshold ε. If the RMSE between the aligned template and rebar point clouds exceeds ε, it indicates insufficient alignment and necessitates corrective action. The correction involves introducing displacement value s along both the positive and negative directions of the outer rebar axis in the template frame, followed by recalculating the RMSE for both cases. The displacement correction is then applied in the direction that minimizes the error. Point-to-plane ICP is subsequently reapplied until either the accuracy requirement is satisfied or the maximum number of iterations is reached. In this paper, the RMSE threshold ε was set to 0.9, and the displacement value s was set to $2d$, where d represents the diameter of the inner rebar. This displacement correction strategy enhances alignment robustness and improves overall registration accuracy, leading to more accurate pose estimations for the rebar tying task.

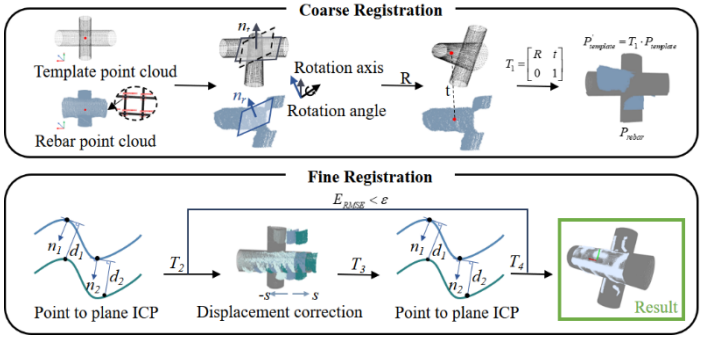

Figure 3. Coarse registration module and fine registration module.

3 Experiment Design

3.1 Experiment Device

The proposed rebar pose estimation method has been integrated into a rebar tying robot developed by our research team, as shown in Figure 4. This system comprises several key components: a 4WD mobile base with a load capacity of 150 kg for enhanced mobility; a 6-DoF robotic arm with a working radius of 1,300 mm for versatile manipulation; and a rebar tying gun as the end effector. Additionally, a 3D camera is configured in an "eye-in-hand" setup, providing a resolution of 1280×1024 and achieving a repeatability of 0.1 mm at a distance of 0.5 m. The industrial PC, operating on Ubuntu 20.04, is equipped with an NVIDIA Ampere GPU and an 8-core ARM Cortex-A78AE CPU, ensuring robust computing capabilities for efficient processing.

Figure 4. Rebar tying robot developed by our research team.

3.2 Experiment Settings

Two experiments were conducted to validate the proposed method. Experiment 1 aimed to test the effectiveness of the proposed coarse-to-fine point cloud registration algorithms for rebar pose estimation, comparing it with other mainstream registration algorithms, such as ICP [15], RANSAC [16], and FGR [17]. All algorithms were implemented using Open3D. To assess the performance of each algorithm in complex scenes, a dataset comprising 3,000 point clouds was created, with 600 point clouds captured at each of the following angles: 0°, 10°, 20°, 30°, and 40°. As shown in Figure 5, the production process involved the following steps: (1) Color maps and depth maps were captured at various angles, with 0° being the ideal camera orientation (Z-axis perpendicular to the rebar plane, X- and Y-axes are aligned parallel to the rebar). Other angles were achieved by rotating around the X-, Y-, and Z-axes. (2) The collected color images underwent preprocessing before being input into the YOLOv8 model for tying point localization. (3) Based on the predicted bounding boxes from the YOLOv8 model and the corresponding depth maps, point cloud models of crosspoint regions were extracted.

Experiment 2 aimed to explore the significance of the proposed visual perception technique by deploying it on a rebar tying robot developed by our team (as shown in Figure 4) and comparing it with other rebar tying methods, including manual tying, handheld tying machine, and other rebar tying robots. To verify the robustness of the proposed method across different scenarios, tying accuracy and efficiency are analyzed through tests involving rebars positioned horizontally, vertically, and inclined, as illustrated in Figure 6.

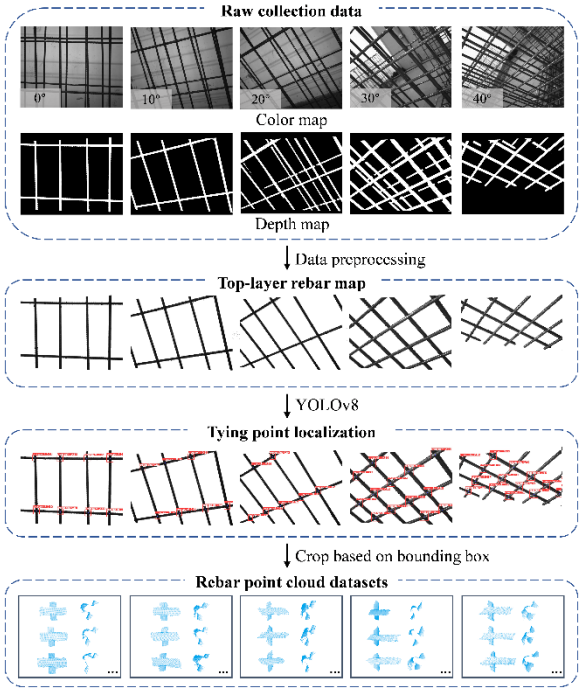

Figure 5. Point cloud model dataset under different shooting angles.

(a) (b) (c)

Figure 6. Different test scenarios: (a) horizontal tying work surface, (b) vertical tying work surface, and (c) inclined tying work surface.

4 Results

4.1 Result of Experiment 1

In Experiment 1, the average RMSE and processing time were utilized to evaluate the performance of four point cloud registration methods. To ensure a fair and reliable comparison of different registration algorithms, an initial translation vector based on the spatial coordinate difference between the tying points in the rebar and template point clouds was provided to each algorithm. This improved both the convergence speed and stability of the registration methods. The experimental results are presented in Table 1. The proposed point cloud registration method significantly reduced the average RMSE error compared to unaligned raw data, effectively addressing texture-less and self-occluding issues during template alignment for rebar pose estimation. Furthermore, the proposed method outperformed other algorithms in registration accuracy across all camera angles and is less affected by camera

angle variations. The superior performance of this method suggests its suitability for the rebar pose estimation task. According to Table 2, the proposed method was slightly slower than ICP, but higher than the other point cloud registration algorithms and still maintained high real-time performance.

Table 1. Average RMSE of different point cloud registration methods (unit: millimeter)

Method	0°	10°	20°	30°	40°
"Raw"	1.039	1.817	3.340	4.913	5.354
ICP	0.522	0.597	0.613	0.812	1.287
RANSAC	1.527	1.751	1.965	2.221	2.532
FGR	2.860	2.893	3.495	4.394	4.637
AnyDirectTying	0.480	0.551	0.526	0.602	0.650

Table 2. Average time consumption of different point cloud registration methods (unit: seconds)

Method	0°	10°	20°	30°	40°
ICP	0.009	0.009	0.010	0.013	0.014
RANSAC	0.098	0.103	0.112	0.119	0.112
FGR	0.032	0.033	0.037	0.039	0.038
AnyDirectTying	0.019	0.024	0.027	0.033	0.034

Given that the ICP algorithm generally outperforms other mainstream methods in terms of accuracy, Figure 7 presents a comparison of the point cloud registration results from the proposed method and the ICP algorithm at various shooting angles. As shown in Figure 7, when the camera angle was at 0°, the performance of ICP algorithm was excellent due to the unaligned raw data being closely aligned, providing an ideal initial state that allowed the ICP algorithm to converge quickly to the correct registration result. However, as the camera angle increased, the accuracy of the algorithm declined. At angle of 10° and 20°, the ICP algorithm tended to fall into local optima rather than achieving the global optimum. This issue was primarily due to self-occlusion, where fewer points were captured from the inner rebar, causing the algorithm to align more readily with the outer rebar while overlooking the misalignment of the inner rebar. This problem became more pronounced when the camera angle reached 30° and 40°, resulting in a rapid decrease in ICP registration accuracy. The proposed method effectively reduces interference by applying an adaptive displacement correction strategy.

In summary, current mainstream point cloud registration methods generally exhibited higher RMSE errors, with some even exceeding those of the unaligned raw data. This discrepancy suggested that existing methods were unsuitable for the task of rebar pose estimation. In contrast, the proposed coarse-to-fine point cloud registration method significantly reduced the RMSE error across different scenarios. This indicated that the proposed method effectively addresses issues related to texture-less surfaces and self-occlusion during template alignment for rebar pose estimation, enabling the robot to accurately perceive the spatial relationship between itself and the tying object, thereby facilitating tying tasks across a broader range of scenarios.

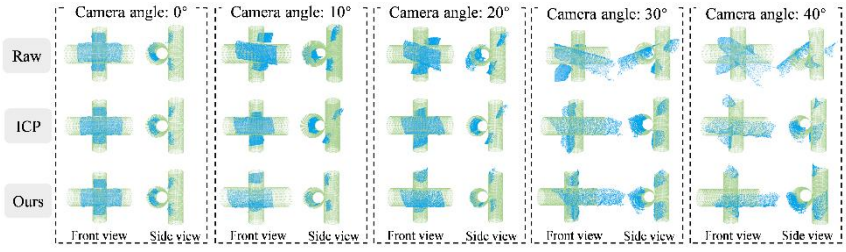

Figure 7. The registration effects of the ICP and the proposed method at different photo angles.

4.2 Result of Experiment 2

To evaluate tying accuracy, 100 rebar crosspoints were tied point by point using the rebar tying robot developed by our research team under different working conditions. As shown in Table 3, the robot achieved a high tying success rate across various working conditions.

In contrast to the visual perception methods of existing robots, which are mainly designed for horizontal rebar mesh and predict only the spatial position of tying points, the proposed method enabled robot to determine the 6-DoF rebar pose in crosspoint region. This capability allows the robot to autonomously perceive the spatial relationship between itself and the tying object, making it capable of performing tying tasks across a broader range of scenarios and demonstrating greater adaptability than existing robotic systems.

Moreover, tying efficiency was analyzed by comparing the average tying time of various tying methods. As shown in Table 4, the average tying time of the rebar tying robot developed in this study was reduced by approximately 39.71% in safe mode and 57.84% in extreme mode compared to manual tying. When compared to handheld tying machine, the robot shortened operation time by approximately 14.58% in safe mode and 40.28% in extreme mode. These results demonstrate that the robot significantly outperforms manual labor by completing more tasks within the same period, thereby boosting construction efficiency. Additionally, the average tying time of our robot was faster than that of other tying robots in extreme mode, although it was slightly slower in safe mode. Nonetheless, the robot maintained a notable overall efficiency advantage.

A further analysis of the tying time components in safe mode revealed that visual perception method accounted for only 0.05 seconds per tying point, just 2.03% of the total tying time. Most of the time was consumed by the execution of the tying action and the movement of the robot arm. This indicates that the slightly lower efficiency in safe mode is primarily due to the mechanical speed of the equipment rather than the performance of the algorithm. Future improvements could focus on deploying the proposed algorithms onto faster, more robust tying robots to enhance their adaptability to multi-directional tying and further improve operational efficiency.

Through the above experiments, it was found that the proposed 6-DoF rebar pose estimation method enabled the robot to perform tying operating across a broader range of scenarios accurately. Additionally, the rebar tying robot deployed with the proposed method demonstrated significant efficiency advantages compared to manual tying and other automatic tying techniques, highlighting the potential of the proposed method to improve construction productivity by guiding the robot towards more efficient and accurate robotic operations.

Table 3. Success rates of our rebar tying robot under different working conditions

Scenario	horizontal	vertical	inclined
Ours	99%	98%	98%

Table 4. Comparison of efficiency of different rebar tying techniques [3,5]

Rebar tying techniques	Average tying time
Manual tying	4.08
Handheld tying machine	2.88
Beijing Institute of Technology	2.34
T-iROBO	2.1
TyBot	2.01
Ours (extreme mode)	1.72
Ours (safe mode)	2.46

5 CONCLUSIONS

Traditional visual perception algorithms for rebar tying robots are often limited to tying objects on horizontal rebar meshes. This study proposes a 6-DoF rebar pose estimation method to guide robotic arms in executing tying operations at arbitrary positions and orientations in 3D space, thereby broadening the application of automated tying technology to various rebar configurations. The key innovations include using a deep learning-based keypoint detection algorithm to extract rebar point data, along with a coarse registration method based on geometric features and a fine registration method utilizing adaptive displacement correction strategy. These innovations effectively address the challenges of rebar pose estimation caused by weak texture and self-occlusion.

Two experiments validated the effectiveness of the proposed algorithm. Experiment 1 demonstrated that the proposed coarse-to-fine point cloud registration method outperformed other mainstream algorithms (ICP, RANSAC, and FGR) in accuracy across different camera angles, achieving an average RMSE of 0.650 mm in complex environments and 0.480 mm in ideal conditions. The algorithm maintains real-time performance, with processing time ranging from 0.019 to 0.034 seconds, demonstrating its capability to handle the challenges posed by the weak texture and self-occlusion in rebar point clouds.

Experiment 2 revealed that the tying robot equipped with the proposed algorithm achieved success rates of 99%, 98%, and 98% for horizontal, vertical, and inclined rebar, respectively, demonstrating improved flexibility and adaptability. The robot also exhibited notable efficiency advantages, completing ties in 1.72 seconds (extreme mode) to 2.46 seconds (safe mode), compared to manual methods and other robots.

In summary, this study enhances the tying capabilities of vision-guided rebar tying robots by developing a 6-DoF rebar pose estimation method, thereby extending their applicability to diverse rebar configurations. This research fills a research gap in 6-DoF rebar pose estimation for robotic rebar tying,

offering an advanced visual perception method that reduces reliance on manual labor. Future work will focus on improving the accuracy and stability of the algorithm, particularly regarding variations in rebar diameter or spacing.

ACKNOWLEDGMENTS

The authors would like to acknowledge the financial support provided by the National Key Research and Development Program of China (Grant No. 2023YFC3806800), the National Natural Science Foundation of China (Grant No. 52308312), the Hunan Province funding for leading scientific and technological innovation talents (Grant No. 2021RC4025), and the Postgraduate Scientific Research Innovation Project of Hunan Province (Grant No. CX20240462).

REFERENCE

[1] C.A. Issa and A. Nasr. An experimental study of welded splices of reinforcing bars. *Building and Environment*, 41(10):1394–1405, 2006.

[2] N. Melenbrink, J. Werfel, and A. Menges. On-site autonomous construction robots: Towards unsupervised building. *Automation in Construction*, 119:103312, 2020.

[3] J. Jin, W. Zhang, F. Li, M. Li, Y. Shi, Z. Guo, and Q. Huang. Robotic binding of rebar based on active perception and planning. *Automation in Construction*, 132:103939, 2021.

[4] Future Robotics Technology Center. Chiba Institute of Technology. On-line: https://furo.org/en/works/t_irobo_rebar/t_irobo_rebar.html, Accessed: 06/08/2024.

[5] B. Cheng and L. Deng. Vision detection and path planning of mobile robots for rebar binding. *Journal of Field Robotics*, 41(6):1864–1886, 2024.

[6] D.-C. Hoang, A.-N. Nguyen, V.-D. Vu, T.-U. Nguyen, D.-Q. Vu, P.-Q. Ngo, N.-A. Hoang, K.-T. Phan, D.-T. Tran, V.-T. Nguyen, Q.-T. Duong, N.-T. Ho, C.-T. Tran, V.-H. Duong, and A.-T. Mai. Graspability-aware object pose estimation in cluttered scenes. *IEEE Robotics and Automation Letters*, 9(4):3124–3130, 2024.

[7] J. Guo, X. Xing, W. Quan, D.-M. Yan, Q. Gu, Y. Liu, and X. Zhang. Efficient center voting for object detection and 6D pose estimation in 3D Point Cloud. *IEEE Transactions on Image Processing*, 30:5072–5084, 2021.

[8] C. De Farias, B. Tamadazte, R. Stolkin, and N. Marturi. Grasp transfer for deformable objects by functional map correspondence. In: *International Conference on Robotics and Automation (ICRA)*, pages 735–741, Philadelphia, PA, USA, 2022.

[9] T. Tang, C. Wang, and M. Tomizuka. A framework for manipulating deformable linear objects by coherent point drift. *IEEE Robotics and Automation Letters*, 3(4): 3426-3433,2018.

[10] Y. Zhu, M. Li, W. Yao, and C. Chen, A review of 6D object pose estimation. In: *2022 IEEE 10th Joint International Information Technology and Artificial Intelligence Conference (ITAIC)*. pages 1647–1655, Chongqing, China, 2022.

[11] C.-M. Lin, C.-Y. Tsai, Y.-C. Lai, S.-A. Li, and C.-C. Wong. Visual object recognition and pose estimation based on a deep semantic segmentation network. *IEEE sensors journal*, 18 (22): 9370–9381, 2018.

[12] A. Aboah, B. Wang, U. Bagci, and Y. Adu-Gyamfi. Real-Time Multi-Class Helmet Violation Detection Using Few-Shot Data Sampling Technique and YOLOv8. In *IEEE/CVF Conference on Computer Vision and Pattern Recognition (CVPR)*, pages 5350–5358, Vancouver, BC, Canada, 2023.

[13] S. Wang, L. Deng, J. Guo, M. Liu, and R. Cao. Automatic Quality Inspection of Rebar Spacing Using Vision-Based Deep Learning with RGBD Camera. In *International Symposium on Automation and Robotics in Construction*, pages 57–64, Lille, France, 2024.

[14] Z. Zou, H. Lang, Y. Lou, and J. Lu. Plane-based global registration for pavement 3D reconstruction using hybrid solid-state LiDAR point cloud. *Automation in Construction*, 152:104907, 2023.

[15] K.-L. Low. Linear least-squares optimization for point-to-plane icp surface registration. Chapel Hill, University of North Carolina, 4(10):1-3, 2004.

[16] M. A. Fischler and R. C. Bolles. Random sample consensus: a paradigm for model fitting with applications to image analysis and automated cartography. *Communications of the ACM*, 24(6):381–395, 1981.

[17] Q.-Y. Zhou, J. Park, and V. Koltun. Fast Global Registration. In *Proceedings of the European Conference on Computer Vision*, pages 766–782, Cham, Switzerland, 2016.